Article type: brief communication

Probing the Surface Loss Probability of Reactive Species in Plasma Polymerization

Robin Dantinne[1*], Philippe Leclère[2], and Damien Thiry[1]

[1] Chimie des Interactions Plasma-Surface (ChIPS), Research Institute for Materials Science and Engineering, CIRMAP, University of Mons, 20 Place du Parc, B-7000 Mons, Belgium.
[2] Laboratory for Physics of Nanomaterials and Energy (LPNE), Research Institute for Materials Science and Engineering, CIRMAP, University of Mons, 20 Place du Parc, B-7000 Mons, Belgium

*Corresponding author
Robin Dantinne, Chimie des Interactions Plasma-Surface (ChIPS), Université de Mons, 20 Place du Parc, B-7000 Mons, Belgium
Email : robin.dantinne@umons.ac.be

Abstract

Plasma polymerization is a promising technique for synthesizing organic thin films, yet its growth mechanism at the plasma-surface interface remains insufficiently understood. Here, plasma polymerization within a three-dimensional "undercut" geometry is investigated as a diagnostic tool to evaluate the apparent surface loss probability β of the film-forming species, closely related to their sticking coefficient. By varying dissipated power and substrate temperature, β is shown to evolve from 0.13 to 0.46, providing new insights regarding the influence of synthesis conditions on 3D film growth and surface reactivity. The latter is significantly influenced by the substrate temperature governing the residence time of the reactive species. Calculated physisorption energies significantly differ between low- and high-power regimes, highlighting the different plasma chemistries.

Keywords: growth mechanism; complex geometry substrate; plasma polymerization; substrate temperature; sticking coefficient; surface loss probability

Abbreviations: PPF, Plasma Polymer Film; **T**s, substrate temperature; $\mathbf{P_{RF}}$**,** power dissipated in the plasma

1 INTRODUCTION

Studied for over 50 years, plasma polymerization is now recognized as a versatile technique for the synthesis of organic thin films due to the exquisite properties of the coatings including a good thermal stability, excellent adhesion to a wide variety of substrates and insolubility in most solvents. Furthermore, these coatings can exhibit a wide range of chemical functions (e.g. -SH,[1,2] -NH_2,[3,4] -OH,[5] -Br,[6] etc.) of interest for a ever-growing variety of applications such as the immobilization of biomolecules[7] and the fabrication of antibacterial surfaces[8] or controlled drug release coatings.[9]

Briefly, an organic molecule, called precursor, is vaporized within a deposition chamber and activated in a plasma. Through electron-induced collisions, reactive species, such as radicals and to a lesser extent ions, are formed and condensate on nearby surfaces, forming a solid organic thin coating referred to as a plasma polymer film (PPF). Owing to the complex interplay between the gas phase and surface reactions, PPF presents unique properties compared to conventional polymers, such as the absence of repeating units in the film and, in most cases, a high cross-linking degree.[10,11]

As the physicochemical properties of plasma polymer films are governed by their complex growth mechanism, the latter has been extensively studied over the last decades using two complementary approaches. On the one hand, the macroscopic approach seeks to correlate the evolution of film properties and especially deposition kinetics with the energy delivered per particle.[10,12,13] On the other hand, the microscopic approach was developed to provide a detailed picture of plasma chemistry including the identification and quantification of species as well as the determination of the flux and energy of ions reaching the surface.[10,14]

Although considerable knowledge has been gained regarding the growth mechanism of PPF, crucial questions remain concerning the surface reactivity of the film-forming species, which is governed by their sticking coefficients. The latter remains particularly difficult to evaluate due to the limited experimental methods available to directly probe plasma/surface interactions. Recently, a few studies examined the formation of plasma polymers on complex geometry substrates, highlighting their potential as a tool for investigating surface reactions of condensing species. [15–17] The main objective was to mimic the growth of plasma polymer films on complex 3D substrates as required in particular for the surface treatment of biomaterials (e.g. scaffold, complex implant).[15,16,18] Among the several 3D designs introduced in the literature, the undercut geometry characterized by a substantial fraction of the substrate shielded from direct plasma exposure appears as one of the most promising.[16,17] Considering such a geometry, charged

particles cannot reach the shielded region and the plasma polymer growth is governed by diffusion and reaction of neutral film-forming species within the recessed area, excluding ionic contribution to the film growth.

Undercut substrates have been used to compare plasma polymer growth considering various precursors (i.e. HMDSO, HMDSO/O_2 and C_2H_4/CO_2 mixes) yielding valuable information on the surface reactions of film-forming species.[16,17]

Built on this approach, this work reports on an original and simple method to determine the apparent surface loss probabilities of the film-forming species, closely related to their sticking coefficient, and crucial for a molecular-level understanding of plasma polymer growth. Allyl alcohol is selected as a model precursor. Furthermore, the influence on the surface loss probabilities of the power and the substrate temperature identified as key tuning parameters for the plasma polymerization process is also discussed.

2 EXPERIMENTAL SECTION

2.1 Reagents

2-propen-1-ol (99%, Sigma-Aldrich), which will be referenced as allyl alcohol, was used as received on complex geometry substrates (described in the next section). Prior to their introduction in the plasma chamber, the substrates were cleaned with 1-isopropanol three times and dried under a nitrogen flow.

2.2 Complex geometry substrate : “undercut”

A scheme of the "undercut" geometry is presented in Figure 1. Undercut substrates were assembled using 525 µm thick Si wafer pieces : the bottom and top pieces were separated by 3.05 mm with a spacer (stainless steel nuts), shielding part of the bottom Si piece from the plasma and the ion bombardment. Its edge aligned with the edge of the top Si wafer, another Si wafer was placed at the bottom, covering the plasma-exposed part of the substrate. The goal of this Si piece is to prevent low-angle ions from reaching the plasma-shielded zone by extracting them with the electric field at its edge.[17] The side openings of the structure are closed with tape.

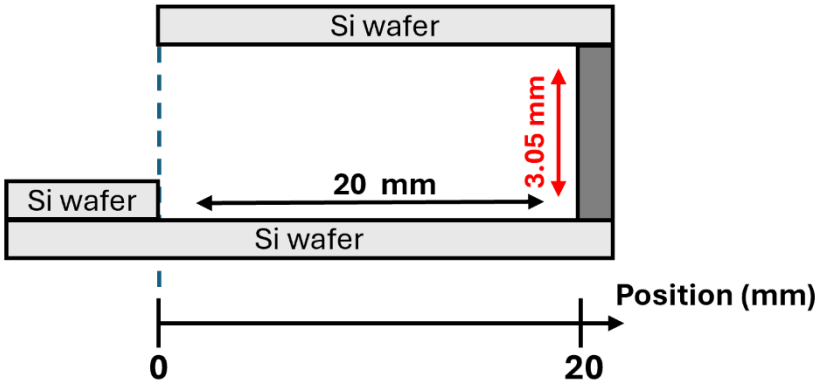

FIGURE 1. Side-view of the undercut geometry made of Si wafer to study the growth mechanism of PPF on a plasma-shielded substrate.

2.2 Plasma polymerization method

Plasma polymer film growth was carried out in a metallic deposition chamber (65 cm in length and 35 cm in diameter) with a residual pressure of less than 2.10^{-6} mTorr. The vacuum was ensured by a combination of turbomolecular and primary pumps. A more detailed description of the plasma chamber can be found elsewhere.[1] Briefly, the reactor consists in an internal one-turn inductive copper coil (10 cm in diameter) cooled with water connected to an Advanced Energy Radiofrequency (13.56 MHz) power supply with a matching network. For all the experiments, the precursor flow was maintained at 10 sccm and the distance separating the substrate from the coil was fixed at 10 cm. The working pressure was 40 mTorr and was controlled during the process with a throttle valve connected to a capacitive gauge. The substrate temperature (T_S) was controlled by a combination of liquid nitrogen flow in the manipulator (for cooling) and electrical resistances in the substrate holder (heating) coupled with a thermocouple, also inside the substrate holder. This system allowed to control the temperature with a precision of ±1°C. Before each deposition, the substrate temperature was stabilized for 30 minutes to ensure the thermal equilibrium between the silicon substrate and the heating/cooling system.

The power dissipated in the plasma (P_{RF}) was either 40W or 80W, associated with a capacitive or inductive allyl alcohol-based plasma, respectively.[1,19] Both modes exhibit important differences, especially in terms of plasma density. This particular feature of ICP discharges is advantageous as, using a single experimental configuration, the plasma polymerization process can be investigated in a large range of electron density.[1] Low-power PPF were deposited with a substrate temperature of 10°C, 23°C or 45°C while high-power coating were obtained for T_S = 45°C, 65°C, 90°C or 120°C.

2.3 Thickness measurements

The deposition profile has been acquired by scratching the coating surface with a scalpel blade and measuring the depth of the produced step by AFM measurement using Peak Force Tapping mode operated on a Bruker AFM ICON Dimension equipped with a Nanoscope 6 Controller. The AFM tips were NCHV-A probes supplied by Bruker with a spring constant k of ± 40 N/m. The section analysis was done by using NanoScope Analysis 3.0.

3 RESULTS AND DISCUSSION

3.1 Results

The deposition profiles are presented in Figure 2, highlighting the different growth of the PPF inside the undercut as a function of the P_{RF} and T_S. For all conditions, the thickness decreases as a function of the distance from the undercut entrance. Considering low-power plasma (Figure 2a), the profile is significantly influenced by the thermal conditions of the substrate in contrast to coatings synthesized at high power presenting a similar thickness profile (Figure 2b).

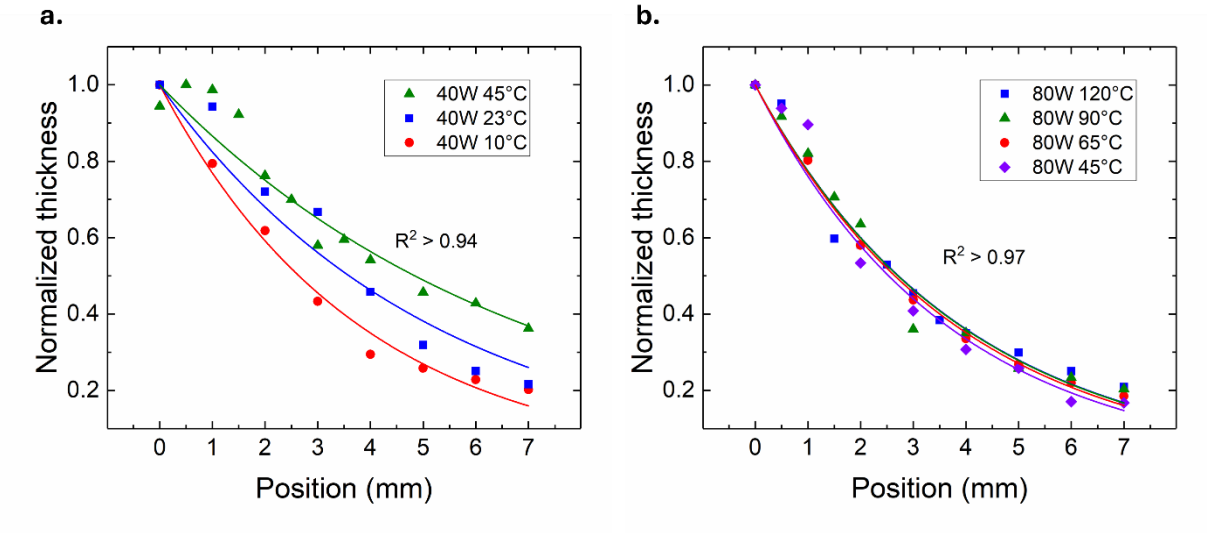

FIGURE 2. Deposition profile inside the plasma-shielded region of the undercut for various substrate temperatures at low (a) and high power (b). The x-axis corresponds to the position relative to the entrance of the covered area (see figure 1). Each thickness profile is normalized with regards to its highest thickness measured inside the undercut. The lines correspond to the fitting of the experimental data using Equation 2.

It should be noted that, in the studied synthesis conditions, no plasma can be created inside the undercut structure to produce reactive species. Indeed, plasma polymerizing discharges have been shown to have a notably low electron density n_e at long distances from the plasma source.[20] Taking values from the literature for a low power plasma ($n_e = 2.10^{13}$ m^{-3} and electronic temperature $T_e = 1.3$ eV),[20] a plasma sheath thickness of roughly 9 mm can be calculated.[21] For an inductive discharge, an increase of one order of magnitude in electronic density can be expected (i.e. $n_e = 2.10^{14}$ m^{-3}), resulting in an estimated plasma sheath of 3 mm.[1,22] Consequently, PPF growth must happen via the diffusion of plasma-activated species from the plasma through the undercut entrance.

Deposition profiles in complex 3D geometry are governed by the surface loss probabilities β, defined as the "probability of losing a reactive particle in a surface collision" :[23,24]

$$\beta = s + \gamma \quad (1)$$

With $r + s + \gamma = 1$

Where r is the probability to reflect the incoming species, s is its sticking coefficient and γ is the probability of forming a volatile stable species (e.g. hydrogen abstraction or radical recombination of two film-forming species).

Although only s contributes to the film growth, both s and γ influence the depletion rate of reactive species. Thus, β instead of s will determine the rate at which the film-forming species density decreases inside a 3D structure. For a high value of β, most of the reactive species are lost after only a few collisions, thus leading to an heterogeneous deposition inside the structure. Inversely, if β exhibits a low value, the density of reactive species inside the structure decreases more slowly, thus leading to a more homogeneous plasma polymer film.

Considering a one-dimensional diffusion model, it has been demonstrated that the concentration profile of a reactive species inside a trench, linearly correlated to the PPF deposition profile, would evolve following Equation 2 :[25]

$$Normalized\ thickness = \frac{C}{C_o} = \frac{cosh\left(\frac{z}{H}\phi\right) + \frac{\phi W}{H2} sinh\left(\frac{z}{H}\phi\right)}{cosh(\phi) + \frac{\phi W}{H2} sinh(\phi)}, \qquad \phi = \frac{H}{W}\sqrt{\frac{3\beta}{2}} \quad (2)$$

Where C and C_o are, respectively, the density of reactive species at a given distance from and at the entrance of the undercut substrate, H and W the length and width of the undercut structure (i.e. respectively 20 mm and 3.05 mm) and β is the effective surface loss probability. Note that the law presented here differs from the original equation as the latter considers that the surface reaction rate is governed by the sticking coefficient instead of the surface loss probability.

Equation 2 successfully described the evolution of the PPF thickness inside the undercut for both low and high power PPF. Figure 3a presents the effective surface loss probability extracted for each set of synthesis parameters. For P_{RF} = 40 W, β evolves from 0.426 ± 0.033 to 0.129 ± 0.017 as T_S increases from 10°C to 45°C, correlating the different deposition profiles observed in Figure 2a. In contrast, β is significantly less affected by T_S at high power, varying only from 0.464 ± 0.064 to 0.403 ± 0.032 over a wider temperature range (45°C to 120°C). This smaller range of β explains the similar profiles obtained for P_{RF} = 80 W whatever T_S (Figure 2b). Those data also correlate PPF deposition profile inside cavity structures (Figure S1).

It is important to note that Equation 2 assumes the reaction of one film-forming species which is obviously not realistic in plasma polymerization where numerous reactive species are formed.

In our case, it could be considered that the apparent surface loss probability deduced from our data is representative of the global surface reactivity of the gas mixture for a given power.

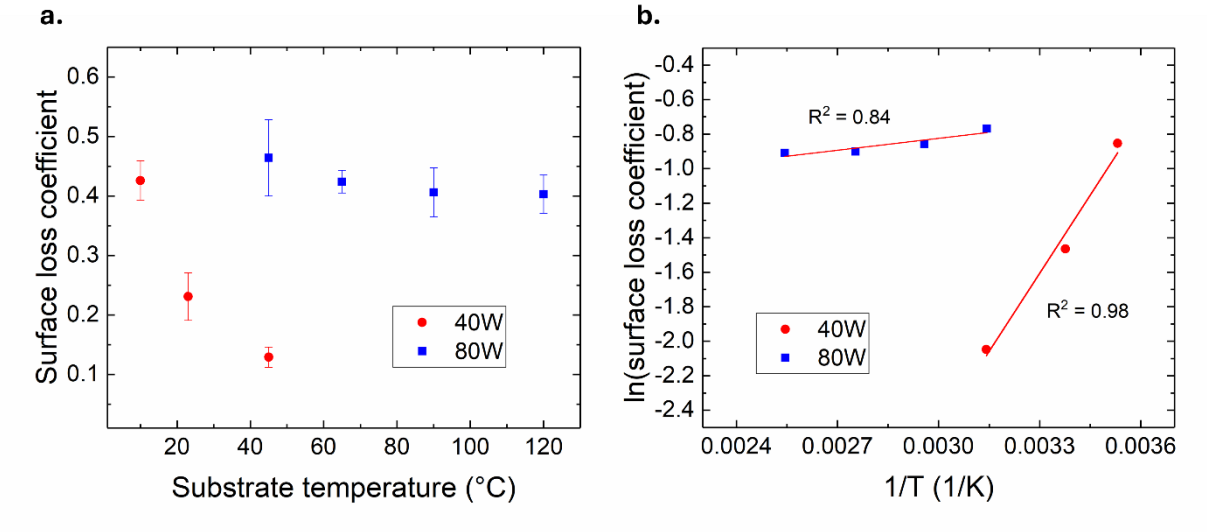

FIGURE 3. (a) Surface loss probabilities for low power (red) and high power (blue) plasma as a function of the substrate temperature. (b) Evolution of ln(β) as a function of the inverse T_S for low power (red) and high power (blue) plasma. Red lines are the linear fit for each power condition.

In order to understand these trends, some fundamental aspects of the molecular growth mechanism of PPF inside a plasma-shielded structure need to be discussed. In the plasma, electronic collisions create reactive species, mainly radicals and to a lesser extent ions. As already mentioned, the ions are excluded from the shielded part of the substrate. Therefore, the diffusion of neutral reactive species is expected to drive the PPF growth inside the 3D structure. These film-forming species adsorb at the interface and form a chemical bond with a surface reactive site through the opening of a double or triple bond or radical recombination, depending on the nature of the reactive site and species.

For a more in-depth description of the molecular growth mechanism, it can be considered that the film-forming species are first physisorbed in a "weakly-adsorbed state". Then, they diffuse on the interface, before reaching a surface reactive site to form a chemical bond and contribute to the film growth.

Considering this mechanism, the residence time τ, i.e. the average time that a particle spend adsorbed on a surface before thermal desorption, will govern the probability of the film-forming species to find a chemisorption site. The probability of other surface reactions, such as the formation of stable volatile species (e.g. through hydrogen abstraction), will similarly be

influenced by the residence time. Thus, β can be expected to be proportional to τ, defined by the following equation :

$$\beta \sim \tau = \tau_o e^{\frac{-E_{phys}}{k_B T_S}} \quad (3)$$

Where τ_0, E_{phys} and k_B correspond to the smallest possible residence time (i.e. the inverse of the vibrational frequency of the surface bond, ~ 10^{-12} – 10^{-13} s), the physisorption energy and the Boltzmann constant, respectively.

According to Equation 3, β is expected to decrease exponentially as a function of T_S. Plotting ln(β) as a function of $1/T_S$ yield E_{phys} (see Figure 3b) : E_{phys} = - 0.26 ± 0.03 eV for low power conditions and – 0.020 ± 0.006 eV for high power plasma. These are typical physisorption values of adsorbed species on a given surface.[26–28] E_{phys} can be seen as an apparent physisorption energy for the reactive species in a weakly-adsorbed state. It should be mentioned that a growth kinetic study determined a similar E_{phys} value than the one of our capacitive plasma (i.e. - 0.23 ± 0.01 eV vs - 0.26 ± 0.03 eV, respectively) considering the same discharge parameters.[29]

The E_{phys} obtained for a capacitive plasma is significantly higher than for an inductive plasma. This supports differences from a chemical point of view in the species reacting at the interface, stemming from the different plasma obtained at low and high power. Indeed, increasing the power dissipated in the plasma is well known to increase the electron density and thus the fragmentation rate inside the discharge.

In a previous work, it was suggested that the radical corresponding to the allyl alcohol molecule missing one hydrogen could be one of the main film-forming species in low power conditions. Consequently, at high power, it could be expected that smaller fragments with a different chemistry would govern the PPF growth mechanism. Furthermore, smaller species are usually associated with a weaker physisorption.[30,31]

4 CONCLUSION

In this study, an innovative approach to determine the apparent surface loss probabilities of film-forming species governing the growth of allyl alcohol plasma polymer is developed considering the undercut geometry as a substrate. Particularly, this work evidences that tuning the dissipated power and the substrate temperature offers a large control over β (i.e. from 0.129 to 0.464 in the conditions studied) and thus on the homogeneity of the coating, paving the way for the use of plasma polymerization in many advanced applications requiring complex 3D

substrates. It should also be highlighted that investigating the influence of various synthesis parameters (e.g. power, substrate temperature, working pressure, etc.) on the undercut deposition profiles allows the extraction of valuable information regarding the plasma/surface interaction and should be considered for future studies aiming at improving our fundamental understanding of the growth mechanism of plasma polymer films.

ACKNOWLEDGMENTS

This publication is supported by the French Community of Belgium ("Communauté française de Belgique") through a FRIA grant. The research at LPNE is partially supported by FRS-FNRS through the PDR and "Grands Equipement" programs.

CONFLICT OF INTEREST

The authors declare no conflict of interest.

DATA AVAILABILITY STATEMENT

The data that support the findings of this study are available from the corresponding author upon reasonable request.

REFERENCES

(1) Thiry, D. Experimental and Theoretical Study of the Effect of the Inductive-to-Capacitive Transition in Propanethiol Plasma Polymer Chemistry. *Journal of Physical Chemistry C* **2013**, *117*. https://doi.org/10.1021/jp400829z.

(2) Aparicio, F. J. Wide Range Control of the Chemical Composition and Optical Properties of Propanethiol Plasma Polymer Films by Regulating the Deposition Temperature. *Plasma Processes and Polymers* **2016**, *13*, 814–822. https://doi.org/10.1002/ppap.201500212.

(3) Denis, L. Deposition of Functional Organic Thin Films by Pulsed Plasma Polymerization: A Joint Theoretical and Experimental Study. *Plasma Processes and Polymers* **2010**, *7*, 172–181. https://doi.org/10.1002/ppap.200900131.

(4) Fally, F. Quantification of the Functional Groups Present at the Surface of Plasma Polymers Deposited from Propylamine, Allylamine, and Propargylamine. *Journal of Applied Polymer Science* **1995**, *56*. https://doi.org/10.1002/app.1995.070560509.

(5) Fahmy, A. Structure–Property Relationship of Thin Plasma Deposited Poly(Allyl Alcohol) Films. *Plasma Chemistry and Plasma Processing* **2011**, *31*, 477–498. https://doi.org/10.1007/s11090-011-9297-0.

(6) Thiry, D. Surface Engineering of Bromine-Based Plasma Polymer Films: A Step toward High Thiol Density Containing Organic Coatings. *Langmuir* **2018**, *34*, 7655–7662. https://doi.org/10.1021/acs.langmuir.8b01045.

(7) Manakhov, A. Cyclopropylamine Plasma Polymers Deposited onto Quartz Crystal Microbalance for Biosensing Application. *physica status solidi (a)* **2014**, *211*, 2801–2808. https://doi.org/10.1002/pssa.201431399.

(8) Sťahel, P. Atmospheric Pressure Plasma Polymerized Oxazoline-Based Thin Films—Antibacterial Properties and Cytocompatibility Performance. *Polymers* **2019**, *11*, 2069. https://doi.org/10.3390/polym11122069.

(9) Bhatt, S. Plasma Co-Polymerized Nano Coatings – As a Biodegradable Solid Carrier for Tunable Drug Delivery Applications. *Polymer* **2013**, *54*, 4820–4829. https://doi.org/10.1016/j.polymer.2013.06.054.

(10) Snyders, R. Foundations of Plasma Enhanced Chemical Vapor Deposition of Functional Coatings. *Plasma Sources Science and Technology* **2023**, *32*, 074001. https://doi.org/10.1088/1361-6595/acdabc.
(11) Cossement, D. Chemical and Microstructural Characterizations of Plasma Polymer Films by Time-of-Flight Secondary Ion Mass Spectrometry and Principal Component Analysis. *Applied Surface Science* **2015**, *355*, 842–848. https://doi.org/10.1016/j.apsusc.2015.07.066.
(12) Hegemann, D. Plasma Activation Mechanisms Governed by Specific Energy Input: Potential and Perspectives. *Plasma Processes and Polymers* **2023**, *20*. https://doi.org/10.1002/ppap.202300010.
(13) Hegemann, D. Macroscopic Approach to Plasma Polymerization Using the Concept of Energy Density. *Plasma Processes and Polymers* **2011**, *8*, 689–694. https://doi.org/10.1002/ppap.201000211.
(14) Thiry, D. Plasma Diagnostics for the Low-Pressure Plasma Polymerization Process: A Critical Review. *Thin Solid Films* **2016**, *606*, 19–44. https://doi.org/10.1016/j.tsf.2016.02.058.
(15) Michlíček, M. Deposition Penetration Depth and Sticking Probability in Plasma Polymerization of Cyclopropylamine. *Applied Surface Science* **2021**, *540*, 147979. https://doi.org/10.1016/j.apsusc.2020.147979.
(16) Hegemann, D. Permanent Plasma Surface Functionalization of Internal Surface Areas. *Advanced Materials Interfaces* **2025**, *12*. https://doi.org/10.1002/admi.202400727.
(17) Navascués, P. Polymerization Mechanisms of Hexamethyldisiloxane in Low-Pressure Plasmas Involving Complex Geometries. *Applied Surface Science* **2024**, *645*. https://doi.org/10.1016/j.apsusc.2023.158824.
(18) Guex, A. G. Covalent Immobilisation of VEGF on Plasma-Coated Electrospun Scaffolds for Tissue Engineering Applications. *Colloids and Surfaces B: Biointerfaces* **2014**, *123*, 724–733. https://doi.org/10.1016/j.colsurfb.2014.10.016.
(19) Kortshagen, U. On the E - H Mode Transition in RF Inductive Discharges. *Journal of Physics D: Applied Physics* **1996**, *29*, 1224–1236. https://doi.org/10.1088/0022-3727/29/5/017.
(20) Dhayal, M. Using Heated Probes in Plasma Polymerising Discharges. *Surface and Coatings Technology* **2004**, *184*, 116–122. https://doi.org/10.1016/j.surfcoat.2003.10.005.
(21) Chen, F. F. *Lecture Notes on Principles of Plasma Processing*; Springer US: Boston, MA, 2003. https://doi.org/10.1007/978-1-4615-0181-7.
(22) Lee, J.-K. E–H Mode Transition in Inductively Coupled Plasma Using Ar, O2, N2, and Mixture Gas. *Current Applied Physics* **2011**, *11*, S149–S153. https://doi.org/10.1016/j.cap.2011.04.009.
(23) Hopf, C. Surface Loss Probabilities of Hydrocarbon Radicals on Amorphous Hydrogenated Carbon Film Surfaces. *Journal of Applied Physics* **2000**, *87*, 2719–2725. https://doi.org/10.1063/1.372246.
(24) Keudell, A. von. Surface Processes during Thin-Film Growth. *Plasma Sources Science and Technology* **2000**, *9*, 455–467. https://doi.org/10.1088/0963-0252/9/4/302.
(25) Hong, L.-S. Macro/Microcavity Method and Its Application in Modeling Chemical Vapor Deposition Reaction Systems. *Thin Solid Films* **2000**, *365*, 176–188. https://doi.org/10.1016/S0040-6090(99)01058-5.
(26) Raman, A. S. Energy Trends in Adsorption at Surfaces. In *Handbook of Materials Modeling*; Springer International Publishing: Cham, 2020; pp 1321–1341. https://doi.org/10.1007/978-3-319-44680-6_2.
(27) Horn, K. *Electronic Structure*; ISSN; Elsevier Science, 2000.

(28) De Moor, B. A. Physisorption and Chemisorption of Alkanes and Alkenes in H-FAU: A Combined Ab Initio–Statistical Thermodynamics Study. *Physical Chemistry Chemical Physics* **2009**, *11*, 2939. https://doi.org/10.1039/b819435c.
(29) Dantinne, R. Investigating the Influence of the Substrate Temperature and the Organic Precursor on the Mechanical Properties of Low-Pressure Plasma Polymer Films. *Plasma Processes and Polymers* **2024**, *21*. https://doi.org/10.1002/ppap.202400166.
(30) Tait, S. L. N -Alkanes on Pt(111) and on C(0001)/Pt(111): Chain Length Dependence of Kinetic Desorption Parameters. *The Journal of Chemical Physics* **2006**, *125*. https://doi.org/10.1063/1.2400235.
(31) Brogaard, R. Y. Modeling van Der Waals Interactions in Zeolites with Periodic DFT: Physisorption of n-Alkanes in ZSM-22. *Catalysis Letters* **2012**, *142*, 1057–1060. https://doi.org/10.1007/s10562-012-0870-9.

SUPPORTING INFORMATION

Additional supporting information is available in the online version of this article at the publisher's website or from the author.

Figure S1: (a) Side-view of the cavity geometry with an opening of 2 mm. (b) Deposition profile inside the cavity structure for a high power (blue) and a low power (red) plasma. For each cavity, thicknesses are normalized with regards to the highest thickness measured inside the cavity. Indicated values for β are the ones calculated with the undercut technique described by Equation 2.

FIGURES AND TABLES

FIGURE 1. Side-view of the undercut geometry made of Si wafer to study the growth mechanism of PPF on a plasma-shielded substrate.

FIGURE 2. Deposition profile inside the plasma-shielded region of the undercut for various substrate temperatures at low (a) and high power (b). The x-axis corresponds to the position relative to the entrance of the covered area (see figure 1). Each thickness profile is normalized with regards to its highest thickness measured inside the undercut. The lines correspond to the fitting of the experimental data using Equation 2.

FIGURE 3. (a) Surface loss probabilities for low power (red) and high power (blue) plasma as a function of the substrate temperature. (b) Evolution of ln(β) as a function of the inverse T_S for low power (red) and high power (blue) plasma. Red lines are the linear fit for each power condition.